buildings

MDPI

Article

Numerical Investigations of Reinforced Concrete Slabs Subjected to Contact Explosions

Hrvoje Draganić [1,*], Mario Jeleč [1], Goran Gazić [1] and Sanja Lukić [2]

[1] Faculty of Civil Engineering and Architecture Osijek, Josip Juraj Strossmayer University of Osijek, Vladimira Preloga St. 3, 31000 Osijek, Croatia; gfos@gfos.hr or mjelec@gfos.hr (M.J.); ggazic@gfos.hr (G.G.)
[2] Respect-ing d.o.o., Ilirska St. 27, 31000 Osijek, Croatia; respect-ing@respect-ing.hr or sanja.lukic@respect-ing.hr
* Correspondence: draganic@gfos.hr; Tel.: +385-31-544-675

Abstract: This study examines the behaviour of reinforced concrete (RC) slabs subjected to contact explosions through experimental investigations and numerical simulations. A contact explosive charge field experiment was conducted on a bi-directionally reinforced RC slab to characterise the resulting damage patterns. The experimental findings revealed localised perforation and substantial deformation of the reinforcement bars without bar rupture. A numerical model employing the RHT concrete and Johnson–Cook steel material models was implemented in Ansys Autodyn (v 2023 R2) to replicate the observed responses. Initial verification was carried out against data from the literature, and calibration was performed using the instantaneous geometric strain (IGS) as the erosion parameter. An optimal IGS value of 0.375 was found to reproduce the experimental damage most accurately. Subsequent parametric analyses of the validated models investigated the influence of slab thickness and reinforcement ratios on blast resistance. The results demonstrated that increasing the slab thickness substantially mitigates perforation, while higher reinforcement ratios improve overall structural integrity. This work confirms the reliability of the calibrated numerical models for predicting the response of RC slabs to contact explosions, and it offers valuable insight into the design of blast-resistant structures.

Keywords: reinforced concrete slabs; contact explosions; blast-induced damage; numerical analysis; parameter analysis

check for updates

Academic Editor: Wusheng Zhao

Received: 9 February 2025
Revised: 21 March 2025
Accepted: 24 March 2025
Published: 26 March 2025

Citation: Draganić, H.; Jeleč, M.; Gazić, G.; Lukić, S. Numerical Investigations of Reinforced Concrete Slabs Subjected to Contact Explosions. *Buildings* **2025**, *15*, 1063. https://doi.org/10.3390/buildings15071063

Copyright: © 2025 by the authors. Licensee MDPI, Basel, Switzerland. This article is an open access article distributed under the terms and conditions of the Creative Commons Attribution (CC BY) license (https://creativecommons.org/licenses/by/4.0/).

1. Introduction

Blast loads are extreme accidental loads primarily neglected in standard construction design processes. Including them mostly leads to the need for over-dimensioned structural elements and consequently increased building costs. However, for crucial military or civilian facilities, incorporating blast load considerations into the structure design can be essential to enhance user safety. A common strategy to mitigate blast loads is to create buffer zones by increasing the standoff distance using natural or artificial barriers. However, barriers alone may not be enough. As a result, the detailing of structural elements is adapted to include unique design approaches for different materials like steel, wood, or reinforced concrete (RC). The impact of blast loads on structures can vary based on whether the explosion is areal (spread over an area) or contact (directly against a surface). Areal explosions typically cause a widespread response throughout the structure. In contrast, contact explosions tend to inflict localised damage, often seen as cratering or penetration through the total thickness of an element. Several factors influence the nature of the damage, including the explosive's weight and shape, the thickness of the structural

component, the ratio and arrangement of reinforcement bars, and the grade of concrete used in RC structures.

Several studies investigated the effects of contact explosions on RC slabs, examining both un-retrofitted (plain) and retrofitted elements. Most prior research has focused on evaluating the efficacy of different retrofitting materials in enhancing the blast-resistance capabilities of concrete slabs. Experimental testing on fibre-reinforced concrete (FRC) slabs has been reported in refs. [1–6]. Ohtsu et al. [1] investigated the dynamics of spall failure in FRC slabs due to contact blast loading. As the flexural toughness of FRC improves, there is a significant reduction in both the average diameters and volumes of the spall failure. Ohkubo et al. [2] and Beppu et al. [3] investigated the effectiveness of carbon and aramid fibre sheet reinforcement on the explosive-resistant performance of concrete slabs. In contact explosion tests, the local damage of retrofitted slabs was highly reduced compared with un-retrofitted slabs, where fibre sheet reinforcements prevented concrete slabs from fragmenting. Another FRC implementation is presented in the study conducted by Yamaguchi et al. [4]. The blast resistance of double-layered polyethylene fibre reinforced concrete (PEFRC) slabs composed of precast thin plates was fabricated and utilised for contact detonation tests. Results showed that creating an air cavity of 15 mm between the two layers of the PEFRC slab effectively reduced spall damage, while the air space had no advantage in normal RC. The application of aramid fibre-reinforced concrete (AFRC) under localised blast loading is presented by Gao et al. [5]. Scaled-down RC slabs, AFRC slabs, and aramid fibre-reinforced plastic reinforced concrete (AFRPRC) slabs were designed and fabricated to compare the blast resistance through experimental damage analysis. The results show that AFRC improves the blast resistance of reinforced concrete, but not significantly, relative to ordinary RC slabs. In contrast, AFRPRC slabs maintain good integrity and show better blast resistance. The latest study also indicates a possible application of geopolymer-based seawater sea-sand high-performance concrete (G-SHPC) slabs reinforced with basalt FRP bars in relation to direct contact explosions [6]. Some other studies also indicate the potential for the application of polyurea coatings (PUs) [7,8] or polyisocyanate-oxazodone (POZD) polymer materials [9–11] in blast mitigation.

Several studies investigated elements made of (ultra) high-performance concrete (U)HPC [12–14], emphasising its better performance than normal strength concrete (NSC) through its higher compressive and tensile strength, larger energy absorption capacity, good workability, and anti-abrasion ability. Li et al. [12] conducted an experimental and numerical investigation of HPC and NSC slabs sized 2000 mm × 1000 mm × 100 mm and subjected to a 1 kg TNT contact charge. The experimental investigation reported a reduction in damage on HPC slabs compared to NSC slabs, where punching and spall damage were evident. A numerical simulation of the tested scenario was conducted in LS-DYNA (https://lsdyna.ansys.com/, accessed on 23 March 2025) utilising nonlinear dynamic simulation. The conclusion was that the numerical model could reproduce the structural response of tested slabs based on damage patterns. Further, Li et al. [13,14] experimentally investigated the spallation of RC slabs made of NSC and HSC with dimensions of 2000 mm × 800 mm × 120 mm exposed to a 1 kg contact TNT charge placed at the centre of the slabs. Results show that although HSC enhances resistance against dynamic loads, it fails in a more brittle way than NSC slab, resulting in larger craters and fragments. Steel wire mesh was implemented in the HSC slab, reducing the overall slab damage and managing to dissipate input blast energy by its fracture. The conclusion was that the reinforcement design plays a vital role in the blast load resistance of RC elements. The latest study by Ma et al. [15] indicates the mitigation potential of innovative 3D-printed UHPC elements on contact explosions. Several reinforcing methods, layer thickness ratios, and construction

methods for base materials are investigated. Presented test results prove the feasibility and cost-effectiveness of 3DP-UHPC reinforced normal concrete for protective structures.

The combination of high-strength and fibre-reinforced concrete (HS-FRC) was investigated by Luccioni et al. [16,17]. Tests involved contact explosions using 49 g TNT-equivalent charges and near-field blast loads. The experiments utilised steel fibres of two different lengths, 30 mm and 60 mm, as reinforcement. In tests involving contact explosions, the flexural failure in plain un-retrofitted concrete slabs was characterised by concrete spalling, leading to complete perforation of the slabs. The outcomes indicated that shorter fibres are more effective at mitigating concrete cratering and spalling when compared to longer fibres, provided that the content of the fibres remains the same.

Another aspect that influences RC slab performance is whether contact explosions are in the air or underwater. Corresponding experiments of RC slabs to an underwater explosion are limited and are presented in refs. [18–20]. The results indicated that the damage inflicted on RC slabs by underwater explosions was considerably more significant than that from blasts in the air with the same amount of explosive material.

Most previous studies focused on retrofit applications, even though most existing RC structures are not retrofitted. Investigations on the response of such rectangular plain and reinforced concrete slabs subjected to contact explosion are shown in refs. [21–23]. Dua et al. [21] conducted an experimental study on the response of rectangular plain and RC slabs subjected to a contact explosion of a 500 g TNT charge. A finite element model in LS-DYNA was developed and validated with the experimental results. The contact explosion led to slab perforation and extensive cracking in the remaining portions. Notably, while the reinforcement in all slabs experienced bending, it did not shear. The research highlighted that the reinforcement ratio of an RC slab influences the contact explosion resistance due to the confinement effect. Cai et al. [22] investigated the size effect on RC slabs under a direct contact explosion. The results indicated that the explosion size effect was observed in the specimens of smaller sizes, which had less bottom spalling damage even if the upper crater size was approximately the same proportion. An analytical study of local damage on concrete slabs subjected to a contact explosion is shown by Yue et al. [23]. Dynamic behaviour was defined through the concrete rigid–plastic model. The expression for slab threshold thickness depending on spall and perforation was validated by the numerical simulation of a 50 g TNT contact charge on a concrete slab performed in Ansys Autodyn.

Numerical simulations are widely used to predict the response of RC structures to blast or impact loads, including the effects of fracture and the spalling of concrete. An erosion model can consider these effects by removing the elements that have reached specific criteria from the calculation. This approach represents a numerical tool to avoid significant distortion of Lagrange meshes. A review of different erosion criteria and limits used to simulate concrete under blast loads is presented in ref. [24]. The effect of the erosion limit on damage results and the dependence on the material's properties, mesh size, and scaled distance are discussed. However, its application to the simulation of a physical phenomenon requires calibration with experimental results. Another approach based on an arbitrary Lagrangian Eulerian-FEM-smoothed particle hydrodynamics (ALE-FEM-SPHs) coupling method is employed to predict the spalling damage of an RC slab subjected to a blast load [25,26]. This method avoids erosion of the elements and shows a good agreement in terms of the spalling area of the slab, the fragment velocity, and the fragment size distribution for predicting the blast fragments of concrete structures.

The presented study intends to investigate the effect of the contact explosion on un-retrofitted RC slabs. A numerical erosion model was utilised to simulate the experiment and obtain the approximate damage compared to the actual damage. In the first step, preliminary modelling and model verification were performed according to experimental

and numerical results from the literature. The verified model was validated based on the authors' experimental results in the next step. Validation was based on the calibrated instantaneous geometric strain (IGS) used as an erosion parameter. The calibration process indicates a strong influence of the IGS value on damage patterns and deformation values. Finally, a validated model was used for additional parametric analysis to investigate the different reinforcement ratios and slab thicknesses on the overall slab behaviour under a contact explosion.

2. Preliminary Numerical Modelling and Verification

A numerical model of a field-tested RC slab was designed and simulated using Ansys Autodyn [27]. It is a hydrocode software providing high computing capabilities for simulating dynamic fluid–structure interaction problems. The software utilises a Euler, Lagrange, or SPH solver. It can combine these different formulations for optimum calculation. Also, it has the potential for parallel computing that enables quicker computations by model decomposition in several domains equal to a number of available processing cores or networked computers. The computation procedure combines the best aspects of both Euler and Lagrange formulations. The Lagrange domain is used for RC slab modelling, while environment (air) and explosives are modelled using the Euler domain. Air overlaps the RC slab to allow effective Euler–Lagrange coupling throughout the dynamic analysis.

2.1. Model Verification

Experimental and numerical results of RC slab damage obtained by Yang et al. [19] were used for model verification. Verifying the model against existing experimental and numerical results ensures greater accuracy in the simulation. Once the model was verified, a similar approach—based on Yang's model creation procedure—could be applied to the experiment of Draganić et al. [28]. This allows for fine-tuning by adjusting fewer parameters, leading to more accurate simulation results that closely align with the experimental data. This approach is viable because Yang et al. [19] conducted comprehensive experimental and numerical studies on the behaviour of RC slabs subjected to contact explosions in air and water environments.

2.2. Model Description

An RC slab in an air environment with dimensions 1000 mm by 500 mm and 60 mm thickness was subjected to a 210 g TNT contact charge. An RC slab with a mesh size of 5 mm was used, while the air environment was modelled with 10 mm mesh size elements. The numerical model used the RHT material model for concrete and the Johnson–Cook model for steel reinforcement bars. The concrete material part of the slab was modelled as a solid element, while the reinforcement bars were modelled as beam elements. Solid elements are of finite element type Hex8 (SOLID65), i.e., linear eight-node hexahedron elements shaped as an eight-node brick (eight integration nodes on each corner of a finite element). Beam formulations were selected for steel reinforcement to enable the bending behaviour during blast wave interaction with the RC slab due to the lateral loading of reinforcement bars through concrete slab bending. The contact algorithm transforms beam elements into reinforcement bars (LINK8) and allows ideal coupling, enabling an ideally bonded interaction between concrete and reinforcement bars. In the algorithm, reinforcement bars maintain beam characteristics in the analysis. In Autodyn, using a single Euler solver to model both the explosive and the surrounding air is standard. The Jones–Wilkins–Lee (JWL) equation of state typically represents the explosive material, while the ideal gas equation of state governs the air. This unified approach allows the solver to track the detonation

products, their expansion into the air, and the resulting shock waves and fluid–structure interactions [27].

2.3. Material Models

Concrete behaviour was modelled using the RHT material model [29], while reinforcement bar behaviour was modelled using the Johnson–Cook steel model [30]. Based on laboratory results of tested concrete and steel specimens, default material models were modified to obtain more proximate behaviour of an RC slab. One of the material parameters influencing the overall RC slab behaviour and damage, especially considering contact explosion where local damage is very pronounced, is erosion. The physical detachment of failed finite elements characterises erosion, making it an ideal parameter for a more realistic simulation of slab perforation in contact explosion scenarios. An integral part of the RHT material model is a failure by which numerical simulations define and implement erosion. Several erosions based on strain, stress, damage, failure, or minimum time step can be distinguished [24], while commonly used is strain-based erosion.

The RHT concrete model is an advanced plasticity model used for simulating the dynamic loading of concrete, especially for brittle materials. This model combines plasticity and shear damage to restrict the deviatoric stress within the material using a generalised failure surface. It is designed to be modular, allowing for specific aspects of material behaviour to be activated or deactivated, making it highly practical for various applications. Three pressure-dependent strength surfaces are used to describe the state of stress in the RHT concrete model (Figure 1), the elastic limit surface, the failure surface, and the residual strength surface for crushed material. The failure surface and residual surface are stationary, while the elastic limit surface involves a response to internal variables that directly or indirectly include porosity and microcracks. Details regarding all RHT model equations and parameters can be found in ref. [29].

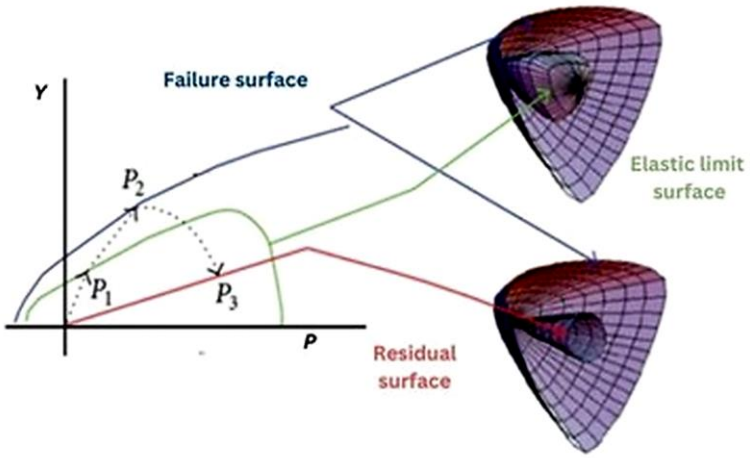


Figure 1. RHT elastic limit, failure, and residual surface.

The Johnson–Cook material model is used to model the reinforcement, which is suitable for modelling the strength behaviour of materials exposed to large deformations, high deformation rates, and high temperatures. It is a bilinear kinematic elastoplastic model [30] represented by the following equation of state:

$$\sigma = \left(A + B(\varepsilon_p)^n\right)\left[1 + Cln\left(\dot{\varepsilon}_p^*\right)\right]\left[1 - (T^*)^m\right] \quad (1)$$

where A is the yield stress, B is the strain hardening exponent, n is the hardening exponent, ε_p is the equivalent plastic strain, C is the strain-rate sensitivity coefficient, $\left(\dot{\varepsilon}_p^*\right)$ is the

dimensionless plastic strain rate, T^* is the homologous temperature, and m is the thermal softening exponent.

The explosive charge was modelled using a TNT material model closely following the used TNT equivalent in Young's experiment. The JWL equation of state that represents explosive material is described with the following equation of state:

$$p = A\left(1 - \frac{\omega}{R_1\chi}\right)e^{-R_1\chi} + B\left(1 - \frac{\omega}{R_2\chi}\right)e^{-R_2\chi} + \frac{\omega}{\chi} \quad (2)$$

where p is hydrostatic pressure, χ is a specific volume $(1/\rho)$, e is specific internal energy, and A, R_1, B, R_2, and ω are constants experimentally determined for several common explosives.

The air is modelled by the equation for the ideal gas. In an ideal gas, the internal energy is a function of temperature, and if the gas is polytrophic, the internal energy is proportional to temperature. The equation of state used is one of the simplest equations of state, and it is as follows:

$$p = (\gamma - 1)\rho e \quad (3)$$

where ρ is the air density, e is specific internal energy, and γ is a constant (ratio of specific heats).

Air is a gaseous material, so it does not have the possibility of transferring stress. As such, no strength law or failure is associated with it. Still, it serves only as a medium for transmitting the shock waves of an explosion caused by detonation to a designated target, i.e., a structure.

Several parameters were modified and compared to the default model to obtain results comparable to experimental damage (Table 1).

Table 1. Default RHT concrete material model parameters and the parameters used by Yang et al. [19].

Parameters	*B*	*M*	D_1	D_2	$\varepsilon_{f,\,min}$	Erosion	A_1 [kPa]	*G* [kPa]	*f*c [kPa]	Tensile Failure
RHT [29]	1.60	0.6	0.04	1	0.01	Geometric strain—1.5 Instantaneous/ Plastic strain/ Timestep/ Failure	3.53×10^7	1.67×10^7	35,000	Hydro/ Principal Stress/ User failure
Yang et al. [19]	+	+	+	+	+	Geometric strain—0.5 Instantaneous	+	1.70×10^7	38,000	Hydro

Note: + denotes the same parameter value as in the default material model. The material parameters are as follows: *B*—fractured strength constant, *M*—fractured strength exponent, D_1 and D_2—damage constants, $\varepsilon_{f,\,min}$—minimum strain to failure, A_1—bulk modulus, *G*—shear modulus, and f_c—compressive strength.

2.4. Result Comparison

A comparison of RC slab damage obtained by the experimental testing and numerical simulation by Yang et al. [19], and the numerical simulation by the authors is shown in Figure 2. The damage pattern is similar for all three cases, with a perforated RC slab by a contact charge. Perforation is circular with slightly different damage diameters. Contact detonation in the experimental test resulted in a circular perforation of 18 cm diameter, while the back surface had a damaged area diameter of 32 cm. Numerical simulations produced somewhat smaller damaged areas. Yang et al. obtained a perforation of 18 cm to 19.2 cm, while the damaged area of the back surface had a diameter of 29.5 cm. The numerical simulation conducted in this work obtained very similar damage. The perforation diameter was 20 cm, and the diameter of the damaged area on the back surface

was 29 cm. Figure 2 shows the overall damage pattern of the top and back surfaces in numerical simulations conducted in this work and by Yang et al. [19]. Based on the compared damage patterns, the conclusion was that the numerical model is verified for further implementation in the numerical simulation of contact explosions compared to the experimental results presented in the following section.

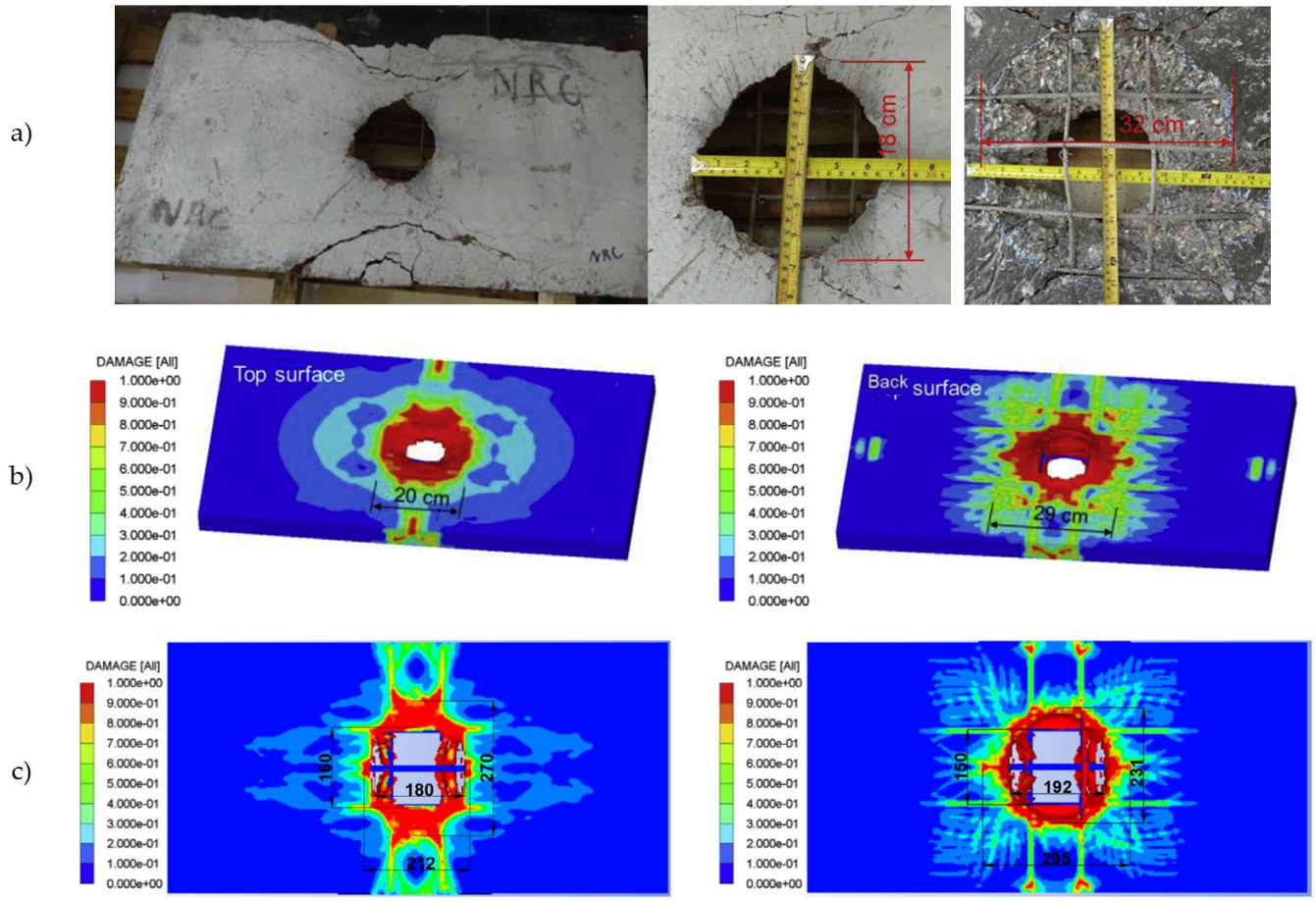


Figure 2. Model verification: (**a**) experimental and (**b**) numerical slab damage by Yang et al. [19] and (**c**) numerical slab damage as simulated in this work. (**a**) Yang et al. [19] experiment with a damaged slab (**left**), top (**middle**), and back surface (**right**). (**b**) Numerical simulation by Yang et al. [19] with top (**left**) and back surface (**right**). (**c**) Numerical simulation by the authors with a top (**left**) and a back surface (**right**).

3. Blast Load Field Tests

A contact explosion was performed on a reinforced concrete (RC) slab at a military testing range. Constitutive materials were laboratory tested following EN standards and testing protocols to acquire the assumed materials parameters for numerical simulations.

3.1. Specimen Description

RC slabs with dimensions of 217 × 100 cm and a thickness of 10 cm were laboratory cast (Figure 3). The built-in reinforcement was a bi-directional steel mesh of 8 mm diameter reinforcing bars spaced at 10 cm in both directions. Steel mesh was placed in two layers, upper and lower, having a distance of 7 cm and a protective layer of 1.5 cm. Based on laboratory testing of concrete cube samples and steel reinforcement mesh, the characteristic compressive strength of concrete was equal to 25.57 MPa, corresponding to strength class C 20/25, and the steel yield and tensile strength were 530 MPa and 607 MPa,

corresponding to strength B500A, respectively. More detailed information regarding the material characteristics and the test setup can be found in Draganić et al. [28].

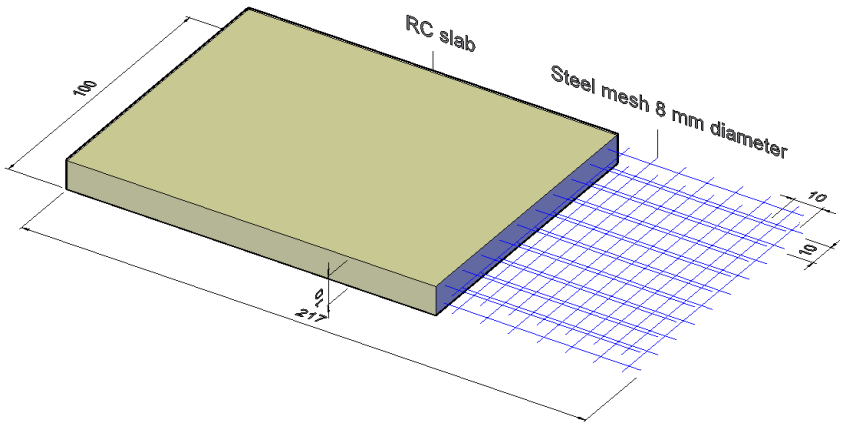


Figure 3. Schematic representation of tested RC slab.

3.2. Test Setup

The slab was tested on a military field range, ensuring all security protocols were followed. Before testing, the research team transported the steel support structure and RC slab to the field range [28]. The RC slab was placed on the steel support structure to secure support rigidity and clamped boundary conditions on two opposite ends (Figure 4). A plastic explosive, designated PEP500, was used in the experiment. It has a TNT equivalent of 1.3, a density of 1.5 g/m^3, and a detonation speed of 7400 m/s. Military personnel moulded the contact charge into a 250 g sphere and placed it at the centre of the top slab surface (Figure 4). A standard lead-azide detonator was placed in the charge centre and was remotely detonated. Potential damage and destruction by high blast pressures and concrete fragmentation prevented us equipping the test specimens with measuring sensors. Overall slab damage was the main parameter to be compared to the numerical results.

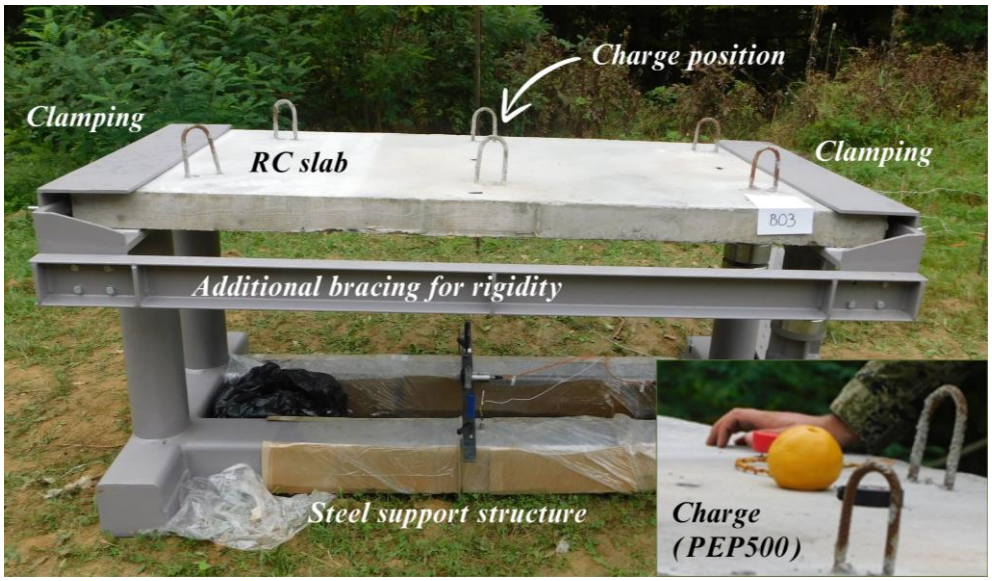


Figure 4. Test setup and contact charge PEP500.

3.3. Experimental Slab Damage

The contact explosion produced slab damage in the form of perforation and scabbing. The perforation was uniform and circular, while the surrounding damaged area was

irregular. Analysis of slab damage distinguished perforation and damaged areas of the upper and lower surfaces, as can be seen in Figure 5. Perforation was characterised by the hole diameter, while the total scabbing square area around the perforation characterised the damaged area. Overall slab damage, if slab cross-section is considered, can be described as an hourglass shape, i.e., the perforation has a funnel shape with a broader upper damage surface that narrows in the middle portion of the section. As perforation continues through slab thickness, it widens and consequently results in more pronounced damage at the lower surface than on the upper, i.e., the damaged area is more extensive. The perforation diameter was 18 cm, corresponding to approximately two "reinforcement mesh openings", while the damaged area was 791 cm^2 and 1540 cm^2 for the upper and lower surfaces, respectively. The wider slab area around the perforation showed extensive cracking on the bottom slab surface; however, after close inspection, it was determined that there were no critical cracks based on which the slab could be characterised as failed. Furthermore, a previous study on the post-blast load-bearing capacity of RC slabs by Jeleč et al. [31] confirmed that their stiffness behaviour remained similar to undamaged RC slabs, with damage localised near the perforation. A lower failure force corresponds to slab damage due to perforation. The steel mesh at the centre of the perforation was deformed but did not rupture. The bars in the steel mesh remained bonded regardless of the severe damage and the blowout of concrete.

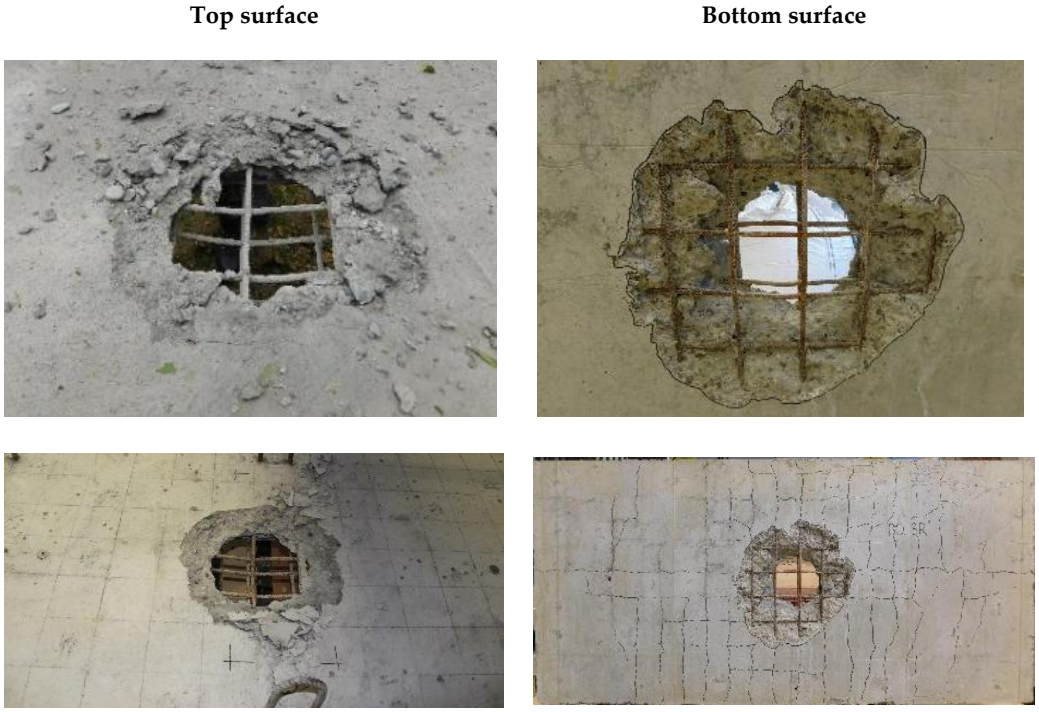


Figure 5. Damage of slab exposed to contact explosion.

4. Calibration and Validation of Numerical Model

4.1. Model Description of Experimental Test

An RC slab is modelled using two parts and materials, as shown in Figure 6. Reinforcement bars in the solid element follow the previously determined layout, with two layers (tension and compression side) having a 7 cm centroid distance. Symmetry enables modelling of only a quarter of the RC slab and consequent blast environment. The reinforced concrete slab, explosive charge geometry, and even the number of reinforcement bars in both slab cross-sections (avoiding symmetry plane through individual reinforcement bars) facilitate symmetry. Symmetry also influenced calculation time, significantly reducing the

calculation time with no crucial loss in accuracy. The clamped boundary condition was simulated by implementing fixed-end supports. Due to symmetry, only one side (shorter) of the slab was constrained. A spherical explosive charge was placed at the centre of the slab in direct contact, resulting in a scaled distance equal to 0 $m/kg^{1/3}$. The explosive material used for simulating the contact blast load on an RC slab was PETN 1.5, corresponding to the plastic explosive used in a field test, PEP500. The detonation point was placed at the centre of the spherical charge and was set as instantaneous, resulting in the instant conversion of explosive material to ideal gas at the start of the simulation. Table 2 lists the material parameters used in the simulation.

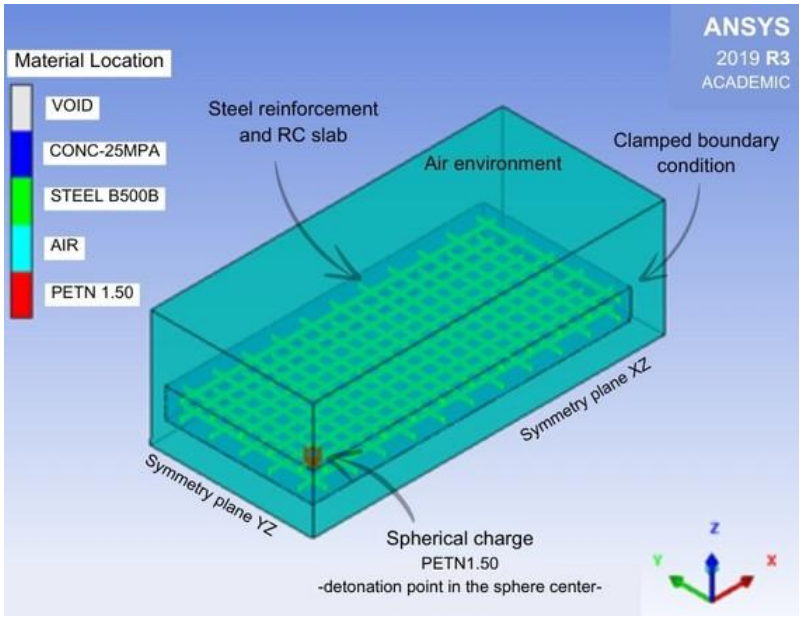


Figure 6. Numerical model of the RC slab.

Table 2. RHT model parameters for simulation.

Parameters	B	M	D_1	D_2	$\varepsilon_{f,\,min}$	Erosion	A_1 [kPa]	G [kPa]	fc [kPa]	Tensile Failure
RHT [29]	1.60	0.6	0.04	1	0.01	Geometric strain—1.5 Instantaneous/ Plastic strain/ Timestep/Failure	3.53×10^7	1.67×10^7	35,000	Hydro/Principal Stress/User failure
Draganic et al. [28]	+	+	+	+	+	Geometric strain—0.375 Instantaneous	+	1.70×10^7	25,570	Hydro

Note: + denotes the same parameter value as in the default material model.

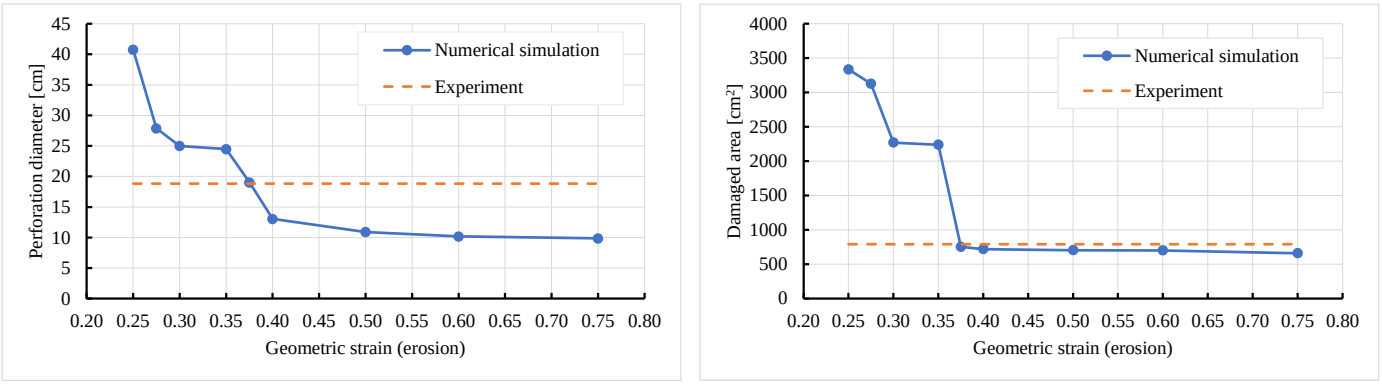
4.2. Simulation Results

Numerical simulations of the RC slab subjected to the contact explosion were performed by varying the erosion parameter. The model implemented erosion governed by instantaneous geometric strain. Geometric strain quantifies the deformation of the material under applied loads, and its instantaneous value reflects the current state of strain at a particular time step in a dynamic simulation. Autodyn calculates the instantaneous geometric strain within each finite element during the simulation. Depending on the material's response to the applied forces, this strain could be axial, shear, or volumetric. Before the simulation, the user must define an erosion criterion based on a threshold value for geo-

metric strain. This threshold is the maximum allowable strain the material can experience before being regarded as failed. If an element exceeds this strain threshold, the simulation considers it failed and removes it from further simulation. This removal is instant in terms of the simulation's time frame, thereby mimicking the real-world phenomenon where a material would fragment or be removed upon reaching its failure strain. The value of geometric strain was varied to obtain more accurate numerical results concerning slab damage. Following previously conducted model verification with the implemented Yang et al. material parameters, the adopted value for geometric strain as an erosion criterion was 0.5. The numerical simulation produced a slab perforation diameter smaller than the experimental results, so additional simulations used the values of 0.75, 0.6, 0.4, 0.375, 0.35, 0.3, 0.275, and 0.25. The analysis utilised a comparison of the RC slab perforation diameter and damaged area for each implemented geometric strain value to obtain optimal erosion parameters for further analysis. Table 3 shows perforation diameters and damaged areas depending on a geometric strain obtained from numerical simulations and differences regarding experimental tests. Figure 7 shows RC slab damage variability depending on erosion parameters.

Table 3. Perforation diameters and damaged areas from experiment and numerical simulation.

Geometric Strain	Perforation Diameter [cm]			Damaged Area [cm^2]		
	Simulation	Experiment	Relative Difference	Simulation	Experiment	Relative Difference
0.250	40.75	18.83	116.41%	3335.04	790.65	321.81%
0.275	27.88	18.83	48.06%	3126.15	790.65	295.39%
0.300	24.99	18.83	32.71%	2269.11	790.65	186.99%
0.350	24.49	18.83	30.06%	2238.08	790.65	183.07%
0.375	19.04	18.83	1.12%	751.77	790.65	4.92%
0.400	13.05	18.83	30.70%	717.78	790.65	9.22%
0.500	10.91	18.83	42.06%	702.92	790.65	11.10%
0.600	10.18	18.83	45.94%	700.12	790.65	11.45%
0.750	9.87	18.83	47.58%	658.34	790.65	16.73%



(**a**) (**b**)

Figure 7. Slab damage variability depending on erosion parameters. (**a**) Perforation diameter vs. geometric strain. (**b**) Damaged area vs. geometric strain.

4.3. Damage Analysis

The data Table 4 presents provide a comparative analysis of the damage sustained by RC slabs subjected to a contact explosion under identical conditions, with the only variable being the instantaneous geometric strain (IGS) which is used as an erosion parameter. This

study illustrates that selecting lower IGS threshold values leads to more extensive damage across the RC slab. Such settings result in larger perforation diameters and increased volumes of concrete eroded from the slab. However, this pattern of widespread damage does not align well with experimental observations, which predominantly show localised damage around the area where the explosive charge was placed, as can be seen in Figure 8. Conversely, selecting higher IGS threshold values leads to a different damage pattern. In this scenario, the damage tends to be more concentrated, characterised by smaller diameters of damage and less eroded concrete volume. This pattern of focused damage is more in line with experimental findings. The benefit of using higher IGS values lies in achieving damage localisation that mirrors the results observed in experimental results. A comprehensive parametric study is essential, given the variability of observed erosion and damage patterns dependent on the IGS value. This study aims to pinpoint the most effective IGS threshold value that would yield results closely resembling those observed in controlled experiments. Table 3 and Figure 7 highlight that an IGS threshold of 0.375 is optimal as it produces perforation diameters and volumes of eroded concrete most similar to the experimental outcomes.

Table 4. Numerically simulated damage of RC slabs under various values of IGS.

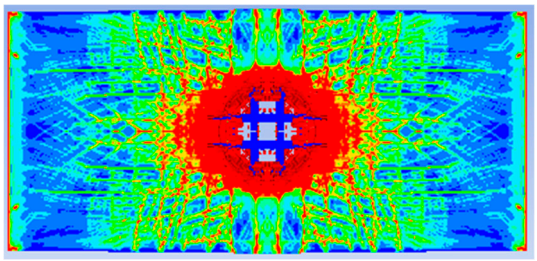
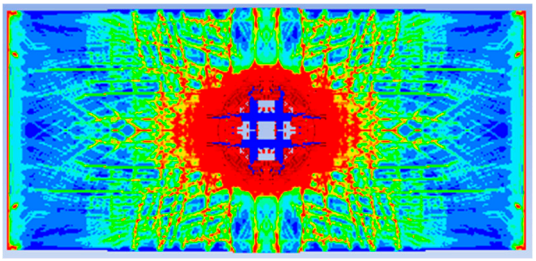
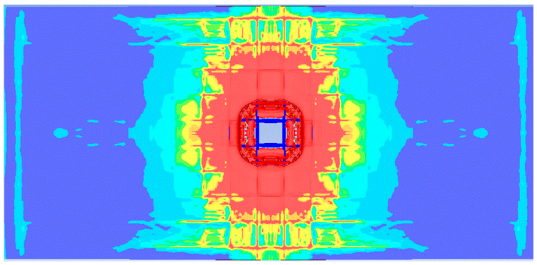
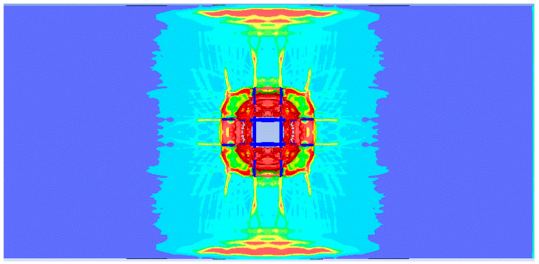
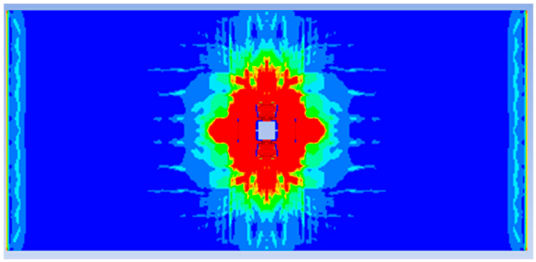
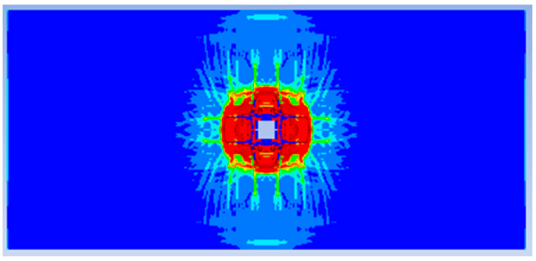
	Top Surface	**Bottom Surface**
IGS		
0.25		
0.275		
0.30		

Table 4. *Cont.*

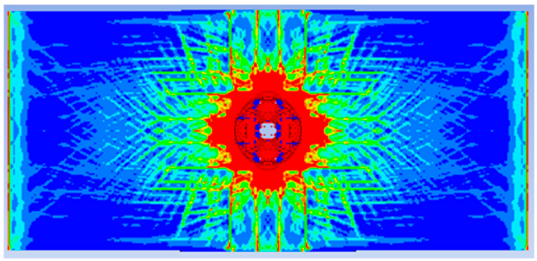
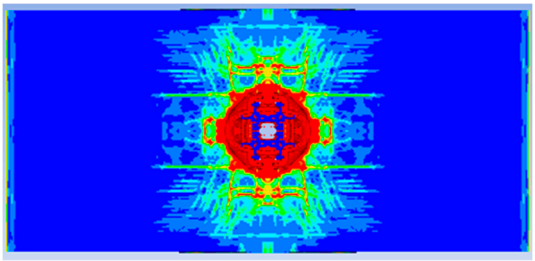
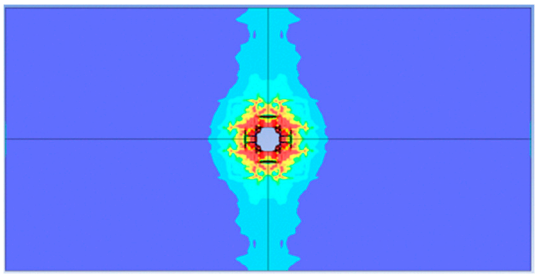
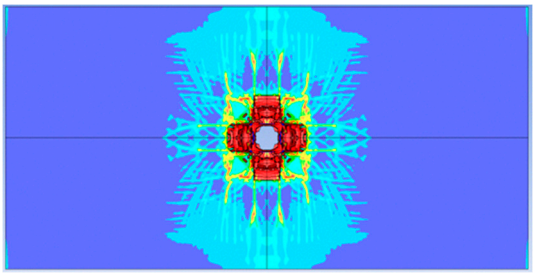
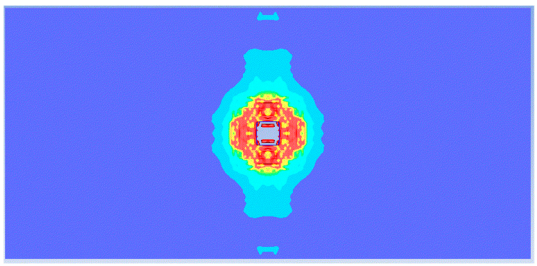
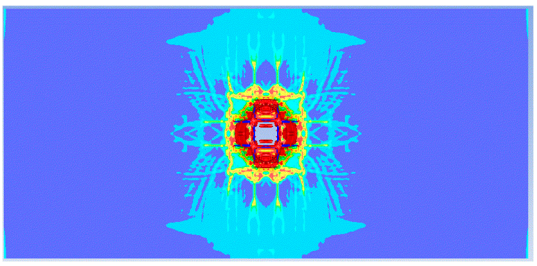
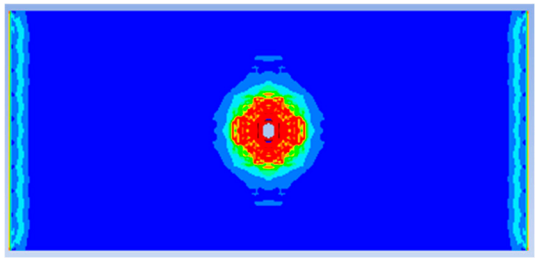
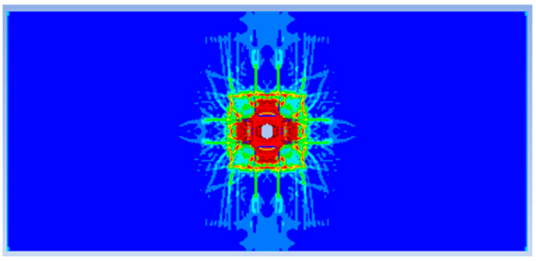
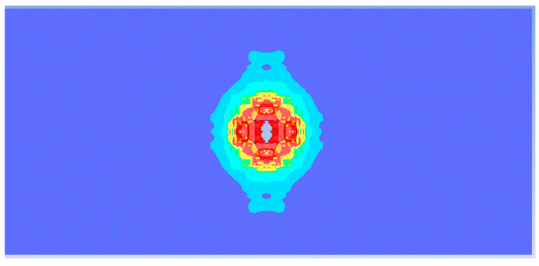
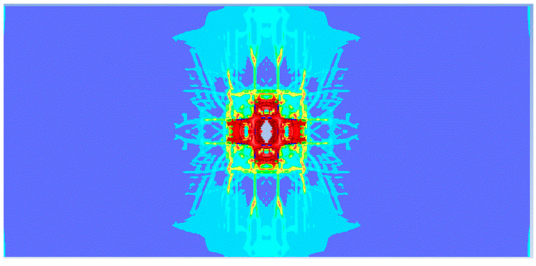
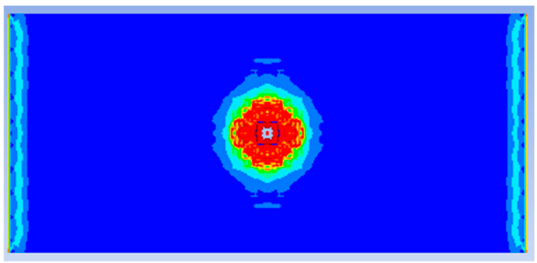
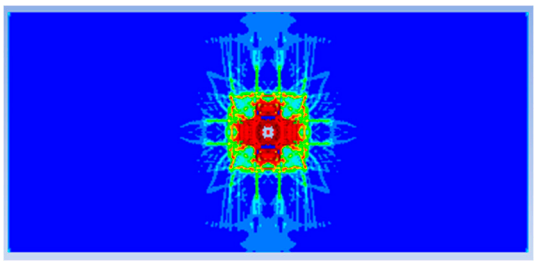
	Top Surface	Bottom Surface
0.35		
0.375		
0.4		
0.50		
0.6		

Table 4. *Cont.*

	Top Surface	Bottom Surface
0.75		

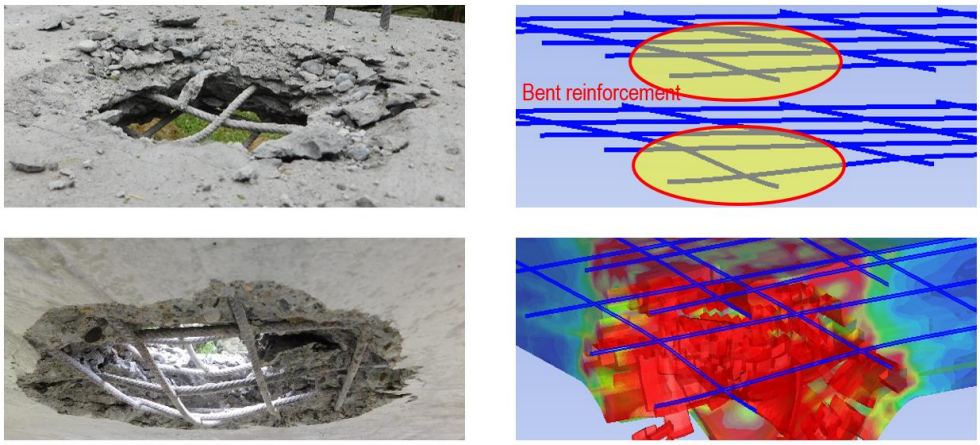


Figure 8. Reinforcement behaviour in experiment and numerical simulation (IGS = 0.375).

Additional observations were made regarding the performance of the slab's reinforcement when exposed to explosive conditions. The slab double-layer reinforcement displayed plastic deformation in regions directly affected by the explosion. This phenomenon is demonstrated by bending the exposed reinforcement bars rather than breaking them, suggesting their ability to undergo plastic deformation under the exerted stress. A uniform response in the reinforcement's behaviour was noted when comparing the outcomes from numerical simulations and experimental tests. This consistency supports the credibility of the simulation model employed in this analysis. Figure 8 shows a close-up of RC slab damage focusing on the reinforcement deformation, with the left from experimental tests and the right from numerical simulations (one-quarter of a slab). The reinforcement has undergone severe plastic deformation without breakage, similar to the experimental tests. Numerical simulations show the reinforcement bending and concrete debris fling out. Also, due to the implementation of the erosion criterion, RC slab perforation can be seen in the middle of the slab. The damage perimeter is jagged due to pronounced square finite elements and their size. Smaller elements could provide an even more proximate damage shape. Still, the further reduction in element size would lead to longer calculation time without a significant increase in result accuracy, i.e., similar perforation diameter with only a "nicer" perforation shape.

Figure 9 overlays a photograph of the RC slab perforation from the experimental test with a numerical visualisation of slab damage, accounting for concrete erosion, to facilitate a more precise comparison between the experimental and numerical damage. The two images show good alignment, demonstrating a reasonable correlation between the experimental and numerical results.

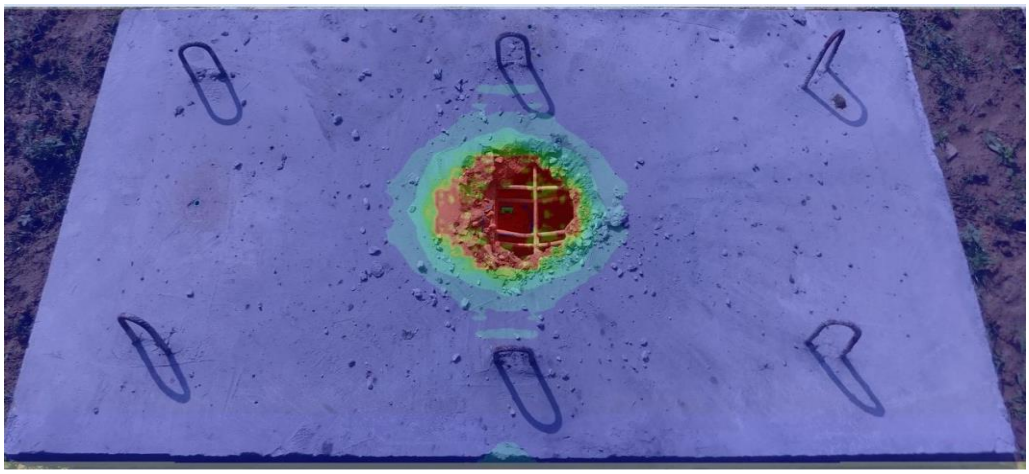


Figure 9. Field test RC slab damage overlaid with numerical simulation (IGS = 0.375).

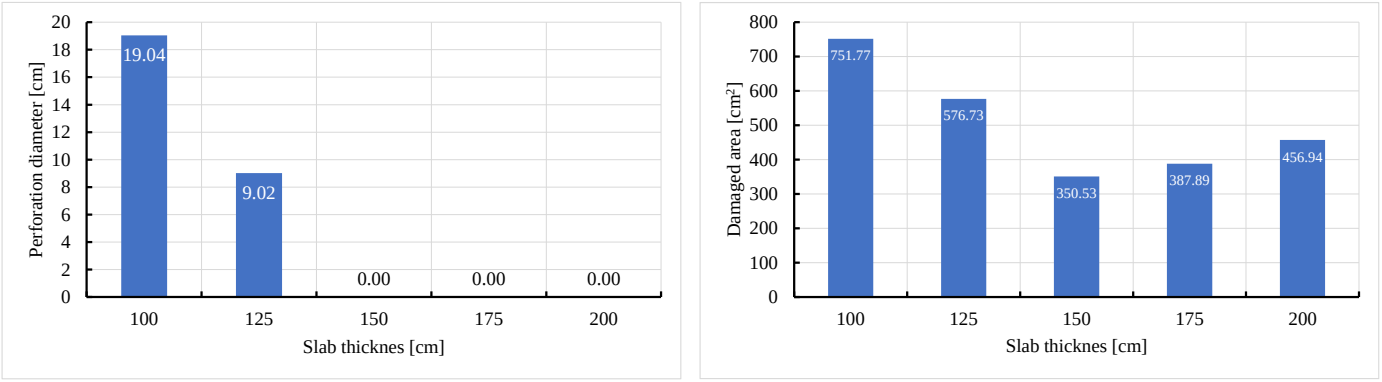
5. Parametric Analysis

After model validation and calibration, additional parametric analysis was conducted to study the influence of different reinforcement ratios and slab thicknesses on the overall slab behaviour under a contact explosion.

The first additional set of models consisted of varying slab thicknesses. Slab thickness was increased from 100 mm to 200 mm in equal steps of 25 mm (125, 150, 175, and 200 mm). The reinforcement area was kept equal in all additional models. Reinforcement distance was increased as slab thickness increased, maintaining an equal concrete cover layer of 25 mm on both sides. All other parameters were kept equal per the validated and calibrated model, i.e., the erosion parameter was kept at 0.375.

The second set of models consisted of varying the reinforcement area by changing the steel mesh bar diameter and reinforcement layout. The referent model, used for modelling experimental testing, consisted of a two-layer steel mesh with 8 mm diameter bars. In comparison, new models consisted of bar diameters equal to 6 mm arranged in one or two layers, whereas in one layer setup, upper reinforcement mesh was removed from the model. A model with a one-layer reinforcement mesh bar diameter of 8 mm was also simulated for comparison. Because of the overall bending action of the blast load on the RC slab, the lower layer reinforcement mesh is kept as a standard reinforcement layout in flooring and roofing slabs if the charge is placed on the upper slab surface. All other parameters were kept equal per the validated and calibrated model, i.e., the erosion parameter was kept at 0.375.

Based on Figure 10 and Table 5, the perforation diameter decreases significantly with an increase in slab thickness—a mere 25 mm increase in thickness results in an almost 50% reduction in the perforation diameter. Further increases in thickness ultimately eliminate perforation, resulting in only surface damage. The damage penetrates approximately one-third of the slab thickness from the top surface. Due to the shock wave's impact and propagation through the slab, significant damage is also observed on the bottom surface, affecting roughly one-third of the slab's thickness. As the slab thickness increases to 175 mm and 200 mm, the penetration of the shock wave diminishes, and its energy dissipates more within the surface layer of the slab.



(**a**) (**b**)

Figure 10. (**a**) Perforation diameter vs. slab thickness, (**b**) damaged area vs. slab thickness; for geometric strain 0.375.

Table 5. Damaged top and bottom surfaces based on slab thickness (constant reinforcement ratio, two layers ø 8).

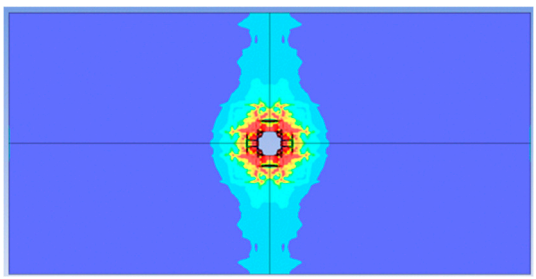
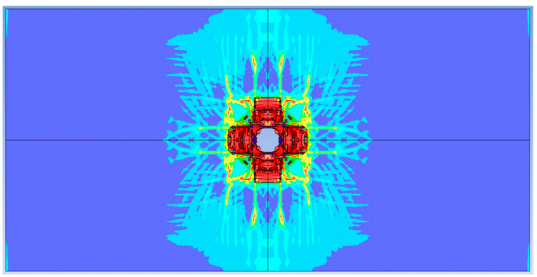
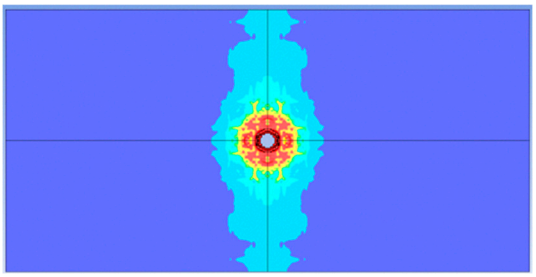
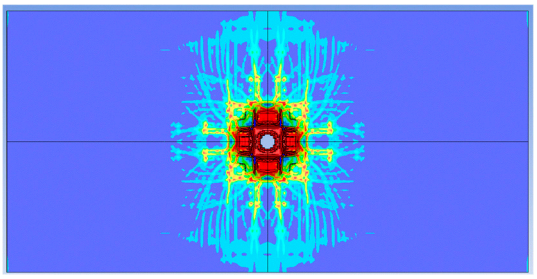
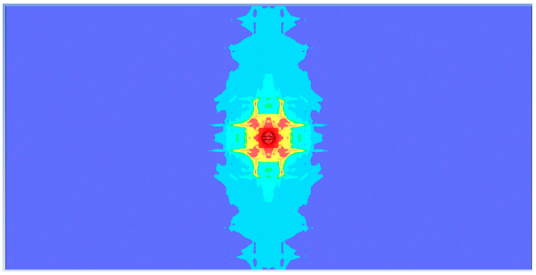
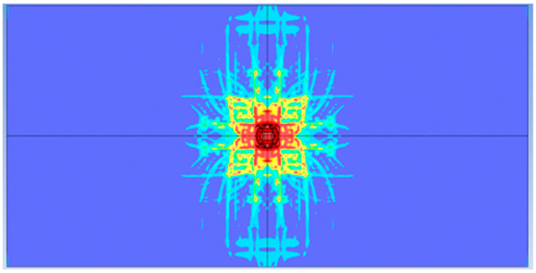
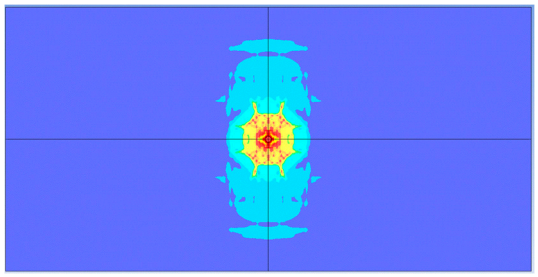
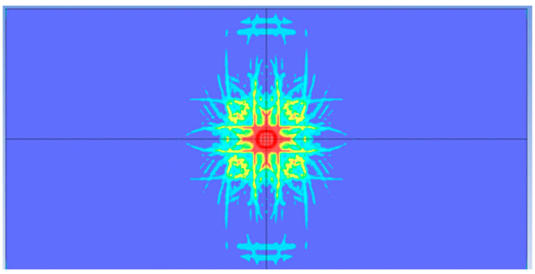
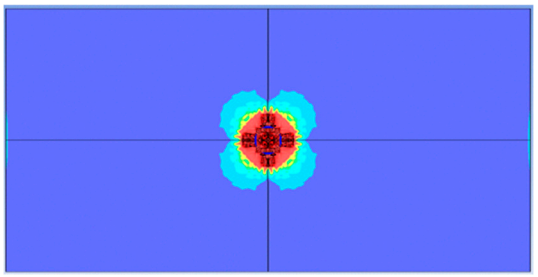
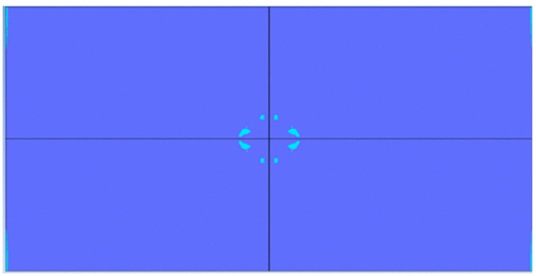
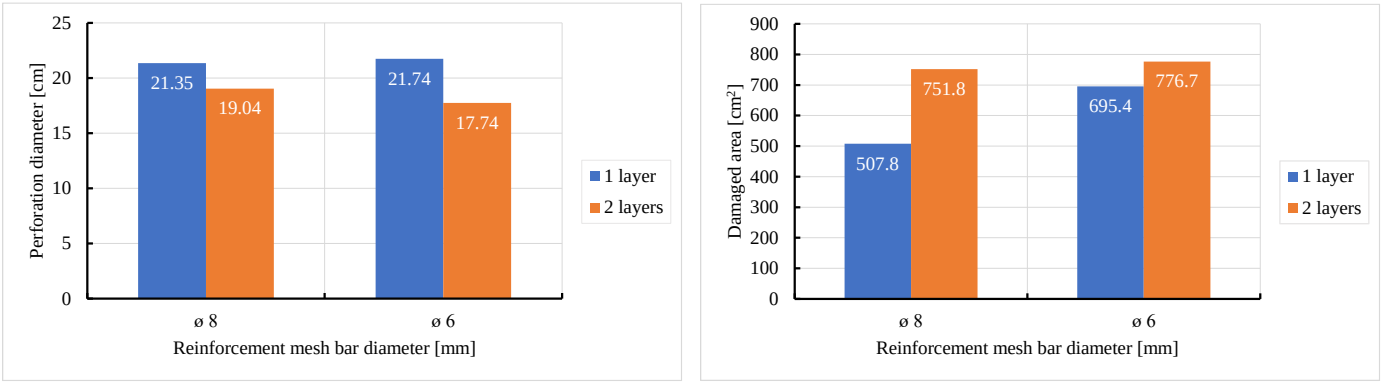
Slab Thickness [mm]	Top Surface	Bottom Surface
		
100		
125		

Table 5. *Cont.*

Slab Thickness [mm]	Top Surface	Bottom Surface
150		
175		
200		

The figures in Table 5 clearly illustrate this trend, where the top surface's damaged area increases with slab thickness. At the same time, the perforation diameter decreases and eventually disappears with a 50 mm thickness increase. Figure 10b further emphasises this progression, showing an initial reduction in the damaged area, followed by an increase in surface damage once perforation is prevented.

Comparing perforation diameters for one and two reinforcement mesh layers reveals that an additional layer reduces the perforation diameter but increases the damaged area. This occurs due to increased slab rigidity, dispersing the blast/shock wave over a larger surface, leading to more extensive concrete flaking and cracking. This trend is shown in 6 mm and 8 mm diameter bar reinforcement slabs, respectively (Figure 11 and Table 6). Consequently, reducing the reinforcement area increases the perforation diameter and overall damage area due to the reduced slab rigidity and resistance to blast wave penetration.



(**a**) (**b**)

Figure 11. (**a**) Perforation diameter vs. reinforcement area, (**b**) Damaged area vs. reinforcement area for geometric strain 0.375.

Table 6. Damaged top and bottom surfaces based on reinforcement layout and area (constant thickness of 100 mm and IGS = 0.375).

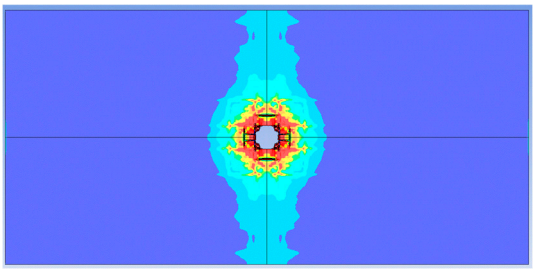
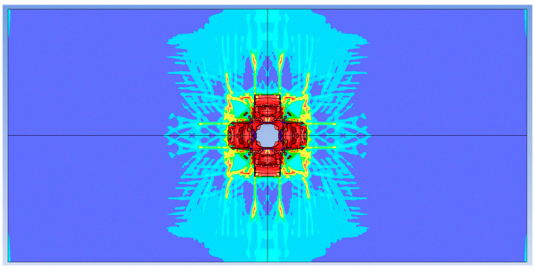
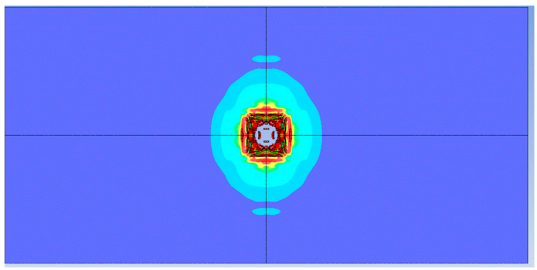
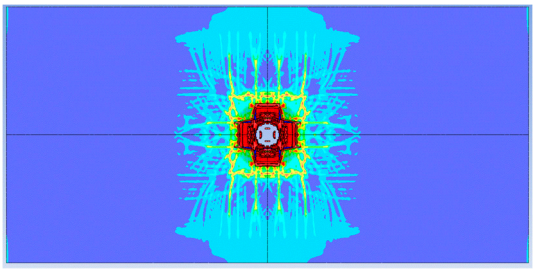
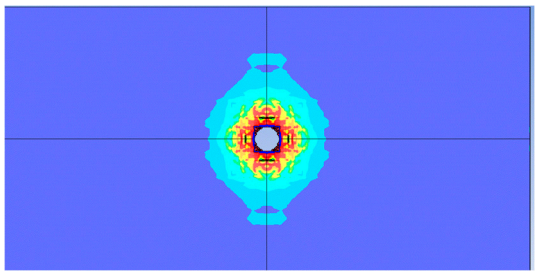
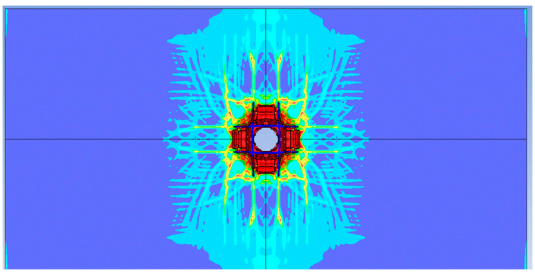
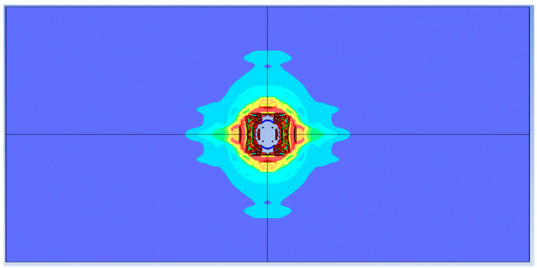
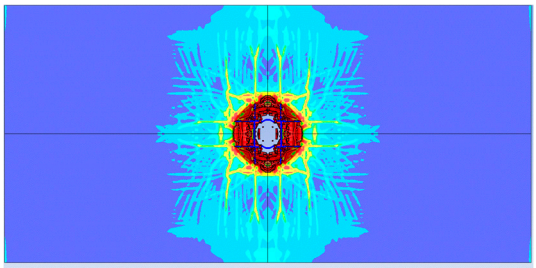
	Top Surface	Bottom Surface
		
2 layers ø8		
1 layer ø8		
2 layers ø6		

Table 6. *Cont.*

	Top Surface	Bottom Surface
1 layer ø6		

6. Conclusions

This study provides an in-depth analysis of the behaviour of un-retrofitted reinforced concrete (RC) slabs subjected to contact explosions through both experimental testing and numerical simulations. The following key conclusions were drawn.

1. Experimental Findings
   - A contact explosion resulted in localised damage characterised by a circular perforation and an hourglass-shaped damage profile without severely compromising structural integrity.
   - Reinforcement bars were bent and experienced significant plastic deformation but retained continuity, confirming their capacity to absorb and redistribute explosive energy without fracturing.
2. Numerical Model Validation
   - The developed numerical model successfully replicated the experimental results when calibrated with an instantaneous geometric strain (IGS) erosion parameter of 0.375.
   - Lower IGS values led to widespread damage, while higher values localised the damage around the contact area, aligning more closely with experimental observations.
   - The only setback observed is that the numerical simulations cannot replicate the identical hourglass shape of the perforation, no matter which parameter is modified. Regardless, if approximate damage in terms of perforation diameter and damaged area is obtained, it is possible to assess the global condition of the structural element after the contact explosion.
3. Parametric Analysis
   - Slab thickness: increasing the slab thickness reduced the perforation diameter drastically and transitioned damage from complete perforation to surface-level damage.
   - Reinforcement area: higher reinforcement ratios (two layers of 8 mm bars) improved blast resistance by reducing perforation but increased the overall damaged area due to greater structural rigidity.
4. Practical Implications
   - The findings emphasise the critical role of reinforcement design and slab thickness in enhancing blast resistance.
   - The validated numerical model offers a cost-effective tool for predicting damage and optimising the design of RC structures for blast mitigation.

Overall, the study confirms that with proper calibration, numerical simulations can effectively predict the response of RC slabs under contact explosions, aiding in the design of safer and more resilient infrastructure. However, the experimental study is limited to a single field-tested specimen, and further investigation is advisable. Additionally, reinforcement strain measurements would provide deeper insights into reinforcement behaviour and support more advanced model validation.

Author Contributions: Conceptualization, H.D., M.J., G.G. and S.L.; data curation, H.D. and G.G.; formal analysis, H.D., G.G. and S.L.; funding acquisition, H.D.; investigation, H.D., M.J., G.G. and S.L.; methodology, H.D., M.J., G.G. and S.L.; project administration, H.D.; resources, H.D.; software, H.D.; supervision, H.D.; validation, H.D. and M.J.; writing—original draft, H.D. and M.J.; writing—review and editing, M.J. and G.G. All authors have read and agreed to the published version of the manuscript.

Funding: The research presented in this paper has been supported in part by the Croatian Science Foundation (HRZZ) under the project UIP-2017-05-7041, "Blast Load Capacity of Highway Bridge Columns", and support for this research is gratefully acknowledged.

Data Availability Statement: All data from this research is accessible by contacting the authors directly.

Acknowledgments: The authors thank the Croatian army for logistical and material support in field blast testing. The authors would also like to thank all the individuals who provided help during the research.

Conflicts of Interest: Author Sanja Lukić was employed by Respect-ing d.o.o. The remaining authors declare that the research was conducted in the absence of any commercial or financial relationships that could be construed as a potential conflict of interest.

References

1. Ohtsu, M.; Uddin, F.A.K.M.; Tong, W.; Murakami, K. Dynamics of spall failure in fiber reinforced concrete due to blasting. *Constr. Build. Mater.* **2007**, *21*, 511–518. [CrossRef]
2. Ohkubo, K.; Beppu, M.; Ohno, T.; Satoh, K. Experimental study on the effectiveness of fiber sheet reinforcement on the explosive-resistant performance of concrete plates. *Int. J. Impact Eng.* **2008**, *35*, 1702–1708. [CrossRef]
3. Beppu, M.; Ohno, T.; Ohkubo, K.; Li, B.; Satoh, K. Contact Explosion Resistance of Concrete Plates Externally Strengthened with FRP Laminates. *Int. J. Prot. Struct.* **2010**, *1*, 257–270. [CrossRef]
4. Yamaguchi, M.; Murakami, K.; Takeda, K.; Mitsui, Y. Blast Resistance of Double-Layered Reinforced Concrete Slabs Composed of Precast Thin Plates. *J. Adv. Concr. Technol.* **2011**, *9*, 177–191. [CrossRef]
5. Gao, Z.; Chen, Y.; Wang, Z.; Li, S.; Wei, W.; Huang, C. Study on the failure effect of aramid reinforced concrete slab under localized blast loading. *Structures* **2024**, *63*, 106292. [CrossRef]
6. Wei, J.; Liu, C.; Liu, J.; Yu, X.; Xu, S.; Su, Y. Investigations on geopolymer-based seawater sea-sand high performance concrete slabs reinforced with basalt FRP bars under direct contact explosions. *Constr. Build. Mater.* **2024**, *411*, 134538. [CrossRef]
7. Shi, S.; Liao, Y.; Peng, X.; Liang, C.; Sun, J. Behavior of polyurea-woven glass fiber mesh composite reinforced RC slabs under contact explosion. *Int. J. Impact Eng.* **2019**, *132*, 103335. [CrossRef]
8. Guo, S.; Liu, F.; Chen, J.; Yang, J.; He, X. Dynamic response and blast resistance mechanism of polyurea coating on RC slab during contact explosions. *Constr. Build. Mater.* **2024**, *411*, 134271. [CrossRef]
9. Wang, W.; Huo, Q.; Yang, J.-C.; Wang, J.-H.; Wang, X.; Gao, W.-L. Damage analysis of POZD coated square reinforced concrete slab under contact blast. *Def. Technol.* **2022**, *18*, 1715–1726. [CrossRef]
10. Wang, W.; Wei, G.; Yang, J.; Liu, F.; Gao, W. Study on antiexplosion performance of reinforced concrete slabs strengthened with POZD coated steel plate under contact explosion. *Eng. Fail. Anal.* **2022**, *140*, 106589. [CrossRef]
11. Wang, W.; Wei, G.; Wang, X.; Yang, J. Structural damage assessment of RC slab strengthened with POZD coated steel plate under contact explosion. *Structures* **2023**, *48*, 31–39. [CrossRef]
12. Li, J.; Wu, C.; Hao, H. Investigation of ultra-high performance concrete slab and normal strength concrete slab under contact explosion. *Eng. Struct.* **2015**, *102*, 395–408. [CrossRef]
13. Li, J.; Wu, C.; Hao, H. Spallation of reinforced concrete slabs under contact explosion. In Proceedings of the 2016 Second Asian Conference on Defence Technology (ACDT), Chiang Mai, Thailand, 21–23 January 2016; pp. 42–45.

14. Li, J.; Wu, C.; Hao, H.; Wang, Z.; Su, Y. Experimental investigation of ultra-high performance concrete slabs under contact explosions. *Int. J. Impact Eng.* **2016**, *93*, 62–75. [CrossRef]
15. Ma, G.; Bai, G.; Wang, L.; Wang, F. Explosion resistance of 3D printing ultra-high performance concrete based on contact explosion tests. *Int. J. Impact Eng.* **2022**, *169*, 104316. [CrossRef]
16. Luccioni, B.; Isla, F.; Codina, R.; Ambrosini, D.; Zerbino, R.; Giaccio, G.; Torrijos, M.C. Effect of steel fibers on static and blast response of high strength concrete. *Int. J. Impact Eng.* **2017**, *107*, 23–37. [CrossRef]
17. Luccioni, B.; Isla, F.; Codina, R.; Ambrosini, D.; Zerbino, R.; Giaccio, G.; Torrijos, M.C. Experimental and numerical analysis of blast response of High Strength Fiber Reinforced Concrete slabs. *Eng. Struct.* **2018**, *175*, 113–122. [CrossRef]
18. Zhao, X.; Wang, G.; Lu, W.; Yan, P.; Chen, M.; Zhou, C. Damage features of RC slabs subjected to air and underwater contact explosions. *Ocean Eng.* **2018**, *147*, 531–545. [CrossRef]
19. Yang, G.; Wang, G.; Lu, W.; Wu, L.; Yan, P.; Chen, M. Experimental and numerical study of damage characteristics of RC slabs subjected to air and underwater contact explosions. *Mar. Struct.* **2019**, *66*, 242–257. [CrossRef]
20. Zhao, X.; Wang, G.; Lu, W.; Yang, G.; Chen, M.; Yan, P. Experimental investigation of RC slabs under air and underwater contact explosions. *Eur. J. Environ. Civ. Eng.* **2021**, *25*, 190–204. [CrossRef]
21. Dua, A.; Braimah, A. Assessment of Reinforced Concrete Slab Response to Contact Explosion Effects. *J. Perform. Constr. Facil.* **2020**, *34*, 04020061. [CrossRef]
22. Cai, R.; Li, Y.; Zhang, C.; Cao, H.; Qi, H.; Mao, J. Size effect on reinforced concrete slabs under direct contact explosion. *Eng. Struct.* **2022**, *252*, 113656. [CrossRef]
23. Yue, S.; Qiu, Y.; Zhang, N.; Wang, M. Analytical study of local damage on concrete slab subjected to a contact explosion. *J. Vibroeng.* **2017**, *19*, 908–929. [CrossRef]
24. Luccioni, B.M.; Aráoz, G.F.; Labanda, N.A. Defining Erosion Limit for Concrete. *Int. J. Prot. Struct.* **2013**, *4*, 315–340. [CrossRef]
25. Wang, Z.; Chen, W.; Hao, H.; Dong, Y.; Huang, Z. Numerical prediction of blast fragmentation of reinforced concrete slab using ALE-FEM-SPH coupling method. *Finite Elem. Anal. Des.* **2023**, *220*, 103948. [CrossRef]
26. Wang, Z.; Chen, W.; Huang, Z.; Hao, H. Numerical study on perforation damage and fragmentation of reinforced concrete slab under close-in explosion. *Eng. Fail. Anal.* **2024**, *158*, 107985. [CrossRef]
27. ANSYS. *Ansys Engineering Analysis System User's Manual*; ANSYS Inc.: Canonsburg, PA, USA, 2019.
28. Draganić, H.; Gazić, G.; Lukić, S.; Jeleč, M. Experimental investigation on blast load resistance of reinforced concrete slabs retrofitted with epoxy resin impregnated glass fiber textiles. *Compos. Struct.* **2021**, *274*, 114349. [CrossRef]
29. Riedel, W.; Thoma, K.; Hiermaier, S. Penetration of reinforced concrete by BETA-B-500 numerical analysis using a new macroscopic concrete model for hydrocodes. In Proceedings of the 9th ISIEMS, Berlin, Germany, 3–4 May 1999; pp. 315–322.
30. Johnson, G.; Cook, W. Selected hugoniots: EOS. In Proceedings of the 7th International Symposium on Ballistics, The Hague, The Netherlands, 19–21 April 1983.
31. Jeleč, M.; Draganić, H.; Gazić, G.; Lukić, S. Post-blast residual static capacity of retrofitted reinforced concrete slabs. *Eng. Struct.* **2023**, *286*, 116161. [CrossRef]

Disclaimer/Publisher's Note: The statements, opinions and data contained in all publications are solely those of the individual author(s) and contributor(s) and not of MDPI and/or the editor(s). MDPI and/or the editor(s) disclaim responsibility for any injury to people or property resulting from any ideas, methods, instructions or products referred to in the content.